RSC Sustainability

ROYAL SOCIETY OF CHEMISTRY

PAPER

View Article Online
View Journal | View Issue

Cite this: *RSC Sustainability*, 2026, **4**, 865

Green initiatives for the synthesis of polyamide monomers: precision fermentation using engineered *Corynebacterium glutamicum* and extraction of purified 5-aminovaleric acid (5AVA) and putrescine

Keerthi Sasikumar,†[a] Volker F. Wendisch *[b] and K. Madhavan Nampoothiri †*[a]

The microbial production of platform chemicals like 5-aminovaleric acid (5AVA) and putrescine presents a green alternative to petroleum-based synthesis, particularly for bio-based polyamides and pharmaceutical precursors. In this study, we employed metabolically engineered *Corynebacterium glutamicum* strains (AVA Xyl and PUT Xyl) for efficient biosynthesis of 5AVA and putrescine in CGXII minimal medium. Initial medium optimization through one-factor-at-a-time (OFAT) experiments identified key components glucose, ammonium sulphate, MOPS, and urea, yielding 4.1 ± 0.21 g per L 5AVA and 0.41 ± 0.01 g per L putrescine. Through successive sub-culturing of PUT Xyl and fermentation, the putrescine titer was improved to 1.82 ± 0.39 g L^{-1}. Further statistical optimization using central composite design (CCD) significantly enhanced the production, achieving 6.0 ± 0.54 g L^{-1} of 5AVA and 6.44 ± 0.33 g L^{-1} of putrescine. Putrescine was concentrated up to 14.3 ± 0.6 g L^{-1} *via* controlled evaporation, and 5AVA was recovered using Dowex 50W-X8 resin in ion exchange chromatography with 84 ± 2% yield. The process design minimized the use of toxic reagents and leveraged water-based, low-energy downstream methods. The integrated approach demonstrates a scalable, environmentally benign route to high value monomers, through green processing strategies.

Received 13th October 2025
Accepted 26th October 2025

DOI: 10.1039/d5su00799b

rsc.li/rscsus

Sustainability spotlight

Conventionally, 5-aminovaleric acid and putrescine are synthesized through petrochemical routes, which involve multiple steps, hazardous intermediates, and high energy consumption. However, producing polyamide monomers such as putrescine and 5AVA from modified microorganisms can significantly advance green chemistry by shifting away from reliance on fossil fuels and reducing the environmental impact of polyamide production. This approach paves the way to utilize renewable resources such as biomass waste and minimizes harmful by-products. Specifically, it enables the development of biodegradable polyamides, promoting a circular economy and reducing plastic waste. In this study we explored a genetically engineered microbial culture which can utilize glucose and xylose (C5). This indicates that the culture is capable of utilizing mixed sugar raw materials like biomass waste and the biosynthetic pathways are streamlined to direct the metabolic flux almost exclusively towards the main products (AVA and putrescine), preventing the formation of any undesired by-products. Thus, further scale up of the process using sustainable and renewable raw materials for producing such value added polyamide monomers will have a huge market for bionylon synthesis and will play a great role in the circular economy. This work emphasizes the importance of the following UN sustainable development goals: UN SDG-12-responsible consumption and production and affordable and clean energy (SDG 7).

1. Introduction

The growing environmental burden of petrochemical-based polymers has accelerated interest in the sustainable biosynthesis of bio-based monomers for use in biodegradable plastics and performance materials. Among these, 5-aminovaleric acid (5AVA) and putrescine have emerged as promising platform chemicals due to their potential applications in the synthesis of polyamides such as nylon-5 and nylon-4,6, respectively. These compounds are not only biodegradable and biocompatible but also align with green chemistry principles, offering lower toxicity and potential circularity in polymer lifecycles.

5AVA ($C_5H_{11}NO_2$) is a linear ω-amino acid containing both amino and carboxyl functional groups, which can be cyclized to valerolactam, a monomer for bio-nylon 5. It also serves as a versatile C5 intermediate for derivatives like glutarate, 5-hydroxyvalerate, and 1,5-pentanediol.[1] In nature, 5AVA is

[a]*Biosciences and Bioengineering Division, CSIR-NIIST, Trivandrum-695019, Kerala, India. E-mail: madhavannampoothiri.niist@csir.res.in*

[b]*Genetics of Prokaryotes, Faculty of Biology & CeBiTec, Bielefeld University, Bielefeld, Germany. E-mail: volker.wendisch@uni-bielefeld.de*

† Current address: Academy of Scientific and Innovative Research (AcSIR), Ghaziabad-201002, India.

a catabolic intermediate in the AMV pathway of *Pseudomonas putida* and is produced *via* L-lysine degradation[2] or cadaverine oxidation. Engineered microbial platforms, such as *Escherichia coli* and *Corynebacterium glutamicum*, have successfully enabled its biosynthesis from renewable carbon sources by heterologously expressing L-lysine monooxygenase (DavB) and 5-aminovaleramide amidohydrolase (DavA).[3–5]

Putrescine (1,4-diaminobutane), the C4 analogue of 5AVA, is a key polyamine involved in DNA/RNA stabilization and cell proliferation. Biosynthetically, it is produced from L-ornithine *via* ornithine decarboxylase (ODC),[6] a pathway highly conserved in prokaryotes and eukaryotes. Putrescine serves not only as a monomer for nylon-4,6 but also as a precursor for spermidine and spermine, essential polyamines in cellular metabolism function.[7] The global market for bio-based putrescine is rapidly growing, projected to reach USD 715.4 million by 2033,[7,8] driven by demand in textiles, automotives, electronics, and bioplastics.[8,9]

Conventionally, 5AVA and putrescine are synthesized through non-renewable petrochemical routes, which involve multiple steps, hazardous intermediates, and high energy consumption.[10] For example, the chemical synthesis of putrescine produces an intermediary compound succinonitrile that is harmful.[11] In contrast, microbial fermentation offers a sustainable and environmentally benign production alternative.[12] Importantly, the integration of renewable carbon sources such as lignocellulosic biomass, rich in xylose and glucose, has become central to green bio-manufacturing.[13,14] Xylose represents one of the most abundant pentose sugars in lignocellulosic biomass, typically contributing about 20–30% of the total carbohydrate fraction in agricultural by-products such as corn stover, wheat straw, rice husk, sugarcane bagasse, and hardwood hemicellulose. While our current study employed commercially available D-(+)-xylose as a model substrate, these lignocellulosic materials are the practical industrial sources of xylose in large-scale bioprocessing. Therefore, establishing the capacity of engineered *C. glutamicum* to metabolize xylose is highly relevant for second-generation biorefineries, where efficient utilization of both pentose (C5) and hexose (C6) sugars is critical to improving process economics.[15] However, microbial utilization of C5 sugars (xylose and arabinose) remains a key bottleneck. Recent advances in *C. glutamicum* engineering have addressed this, including strains capable of producing amino acids,[16] L-homoserine,[17] cadaverine,[18] and 5AVA from lignocellulose-derived sugars and demonstrating co-utilization of xylose and glucose in fed-batch systems.[5,19]

The biosynthetic pathways of AVA Xyl and PUT Xyl strains are streamlined to direct the metabolic flux almost exclusively towards the main products (AVA and Put), preventing the formation of any undesired by-products.[5,20] However, further progress toward industrial application requires a thorough optimization of fermentation parameters, scale up and efficient downstream processing.

In this context, media and process optimization using statistical design of experiments (DoE) is crucial. Initial screening *via* the one-factor-at-a-time (OFAT) approach provides a straightforward method for identifying influential variables, though it does not account for interactions among them. To overcome this, we employed central composite design (CCD), a widely used response surface methodology (RSM) tool that models the nonlinear relationships between process variables, enabling efficient optimization with fewer experiments. CCD is particularly suited for bioprocess development, where multiple interacting factors influence metabolite production.[21,22]

In this study, we report the statistical optimization and eco-friendly recovery of 5AVA and putrescine produced in CGXII synthetic medium. We highlight process enhancements *via* CCD and described a chromatographic method for 5AVA recovery using Dowex 50W-X8 resin, achieving high purity and yield without toxic solvents. Our integrated strategy emphasizes precision fermentation, the low environmental footprint, and alignment with green chemistry objectives contributing to the advancement of bio-based polyamide monomer production through biological means.

2. Materials and methods

2.1. Microorganism and culture conditions

The NA6 strain[23] developed in Prof. Wendisch's lab was transformed with the ITPG-inducible pECXT99A-$xylA_{Xc}xylB_{Cg}$ vector[20] for the overexpression of the xylose isomerase pathway, containing *xylA* (xylose isomerase) from *Xanthomonas campestris* SCC1758 and *xylB* (xylulose kinase) from *C. glutamicum* ATCC13032 for the production of putrescine and denoted as PUT Xyl. The 5-aminovalerate producer strain (pECXT99A-$xylA_{Xc}xylB_{Cg}$) reported earlier[20] was named AVA Xyl. Both these engineered strains, AVA Xyl and PUT Xyl, were used earlier[5] for a proof of concept study for pentose sugar utilization. Here, for detailed fermentation and process optimization studies, seed cultures were made from fresh BHI agar plates supplemented with appropriate antibiotics. For AVA Xyl culture, to induce the promoters of the plasmids pVWEx1-*ldcC*, pEKEx3-*patDA*, and pECXT99A-$xylA_{Xc}$ $xylB_{Cg}$ a final concentration of 1 mM IPTG was added at the time of inoculation. Similarly, the same IPTG concentration is used to induce the promoters, pVWEx1-*speC-gapA-pyc-argB*$^{A49V/M54V}$-$argF_{21}$ and pECXT99A-$xylA_{Xc}xylB_{Cg}$, of the PUT Xyl culture. Unless mentioned otherwise, the fermentation was carried out using CGXII medium [40 g per L glucose, 20 g per L $(NH_4)_2SO_4$, 5 g per L Urea, 1 g per L K_2HPO_4, 1 g per L KH_2PO_4, 0.25 g per L $MgSO_4 \cdot 7H_2O$, 42 g per L MOPS, 0.02 mg per L biotin, 10 mg per L $CaCl_2$ and necessary trace elements] with an initial culture OD (600 nm) of 0.8. The cultures were incubated at 30 °C, 180 rpm and samples were withdrawn every 24 h in the fermentation experiments until 120 h. The antibiotics tetracycline (5 μg mL^{-1}) and kanamycin (25 μg mL^{-1}) and spectinomycin (100 μg mL^{-1}) were added for the AVA Xyl strain and tetracycline (5 μg mL^{-1}) and kanamycin (25 μg mL^{-1}) were used for the PUT Xyl strain.

2.2. Analytical method for the quantification of putrescine and 5AVA

Putrescine and 5AVA were analysed using a Shimadzu UFLC system as described elsewhere[5] with modifications. The system

was equipped with an RF 20A fluorescence detector, set at excitation and emission wavelengths of 348 nm and 450 nm, respectively. Prior to analysis, samples were filtered through 0.22 μm (PALL Life Sciences, USA) membranes, adjusted to pH 10 with a borate buffer (Agilent), and pre-derivatized with *o*-phthaldialdehyde (OPA). Separation was achieved using a Luna® 5 μm C8 column (Phenomenex) with a gradient elution method, employing a 25 mM potassium phosphate buffer (HiMedia, India) and a solvent mixture of acetonitrile (SRL, India), methanol (SRL, India) and water (45 : 45 : 10).

2.3. Single factor optimization

First and foremost, nutrient formulation studies were conducted by a single-factor optimization approach, where we systematically varied the individual variables while all other medium components were maintained at their standard CGXII levels (glucose 40 g L^{-1}, ammonium sulphate 20 g L^{-1}, MOPS 40 g L^{-1}, and urea 5 g L^{-1}). After reviewing the literature, for the AVA Xyl strain, the selected factors and the concentration ranges were glucose (40–70 g L^{-1}), ammonium sulphate (10–40 g L^{-1}), MOPS (10–40 g L^{-1}), and urea (1–5 g L^{-1}). Similarly, for the PUT Xyl strain, glucose (40–80 g L^{-1}), ammonium sulphate (5–25 g L^{-1}), MOPS (5–40 g L^{-1}), and urea (1–5 g L^{-1}) were used.

2.4. Medium engineering and statistical analysis

Experiments were designed to identify the ideal combination of glucose, ammonium sulphate, MOPS, urea, K_2HPO_4 and KH_2PO_4 for both 5AVA and putrescine production in CGXII synthetic medium. Apart from this, xylose was also included as an independent variable for the experiment design as both the AVA Xyl and PUT Xyl cultures possess the genes, xylose isomerase (*xylA*) and xylulose kinase (*xylB*), for xylose utilization. Response Surface Methodology (RSM) with a central composite design (CCD) was used to study the combined effects of these components through 31 and 32 strategically chosen experiments for 5AVA and putrescine production respectively. Two design matrices with various combinations of the independent variables were tested at three levels: −1, 0, and +1 for 5AVA and putrescine production, corresponding to low, medium, and high concentrations, respectively. The input variables were ammonium sulphate (10–20 g L^{-1}), MOPS (20–30 g L^{-1}), urea (2–5 g L^{-1}), xylose concentration (10–30 g L^{-1}) and glucose (20–40 g L^{-1}) and the titer of 5AVA and putrescine respectively served as the response variable for each design matrix. These variable ranges were selected based on the outcomes of single-parameter optimization experiments. The data analysis was performed using Minitab 15 software (Minitab Inc.), where the linear and quadratic effects, as well as potential interactions between the variables, were evaluated. The experimental models for 5AVA and putrescine were validated by arbitrarily selecting five experiments from each design matrix and the response was determined. The model's statistical significance and accuracy were assessed using analysis of variance (ANOVA), with model quality interpreted through *p*-values, the correlation coefficient (R), and the coefficient of determination (R^2).

2.5. Recovery of 5AVA and putrescine from the fermented broth

For the recovery and purification of 5AVA and putrescine, the cell-free fermented broth was charcoal treated and filtered, to obtain a clarified solution by removing the pigments mainly derived from the culture medium and microbial metabolites.

2.5.1. Adsorption and elution of 5AVA by exchange chromatography. The cation exchange resin Dowex 50W-X8 (Sigma, USA) was used for the separation of 5AVA from the fermented broth. The resin was activated prior to separation following the method reported elsewhere.[24] Dowex 50W-X8 resin was washed with deionized water three times, followed by an ethanol (95%) wash and then cleansed with 2 N HCl repeatedly with heating. Finally, the resins were rinsed with deionised water multiple times until the resins attained a neutral pH. The adsorption capacity of the resin was determined by treating varying concentrations (500 mg, 200 mg, 100 mg, 50 mg and 10 mg) of 5AVA (HiMedia, India) with resin. The amount of 5AVA adsorbed per gram of the resin was calculated using eqn (1).

$$q = \frac{A_0 - A_f}{w} \quad (1)$$

where A_0 and A_f are the initial and final concentrations of 5AVA and w is the weight of the resin and q is the percentage adsorption. 10 mg of 5AVA was treated with resin in a wide pH range of 2–8, to find out the ideal pH. To determine the effect of contact time, 1 g (dry weight) of the resin was treated with 10 mg of 5AVA, with constant mixing at pH 4.5 under temperature-controlled conditions at varying time intervals. The elution of 5AVA was monitored with 1 N NaOH with pH 8, 9, 10 and 11.

2.5.2. 5AVA recovery from the fermented broth. The dried Dowex 50W-X8 resins were packed into a glass column (2.5 cm diameter). The pH of the charcoal-clarified cell-free fermented broth was adjusted to 4.5 using 0.1 N HCl and was passed through the column. The column was then washed with two volumes of deionized water, to remove any unbound impurities. This washing step is crucial to ensure that only 5AVA remains bound to the resin, thus improving the purity of the final product. After the required binding time, the elution of 5AVA was carried out using 1 N NaOH and 5AVA was quantified by HPLC.

2.6. Putrescine recovery

The crude fermented broth of PUT Xyl culture which accumulated 6.44 ± 0.33 g L^{-1} of putrescine after 96 h of fermentation was used for the recovery and purification. The clarified cell-free fermented broth was acidified to a pH of 4.5 and centrifuged to remove the precipitated proteins. It was then alkalinized to a near-neutral pH (6–6.5) using 1 N NaOH and subjected to a series of controlled evaporation as per Lee *et al.* (2019)[26] with slight modifications. The rotary evaporator (Heidolph, Germany) was equipped with a condenser, vacuum pump, chiller and water bath. Initially, a mild evaporation (35–40 °C) was done at 340 mbar pressure followed by a second step with a slight increase in the temperature. The temperature of the water bath and pressure were optimized at each step to

concentrate the putrescine in the clarified broth. Eventually, to refine the product a final concentration was done under mild conditions. The concentrated putrescine was analyzed by HPLC and FTIR to confirm the purity. The recyclability of the resins was determined for several cycles.

3. Results and discussion

3.1. Single parameter optimization

3.1.1. Effect of glucose concentration. Being the primary energy source, various concentrations of glucose were used in the CGXII medium to check its effect on the production of 5AVA and putrescine. In the case of 5AVA, a titer of 3.2 ± 0.3 g L^{-1} was obtained after 120 h of fermentation with an initial 50 g L^{-1} of glucose (Fig. 1a). However, further augmentation of glucose to 70 g L^{-1} resulted only in a marginal increase (3.9 ± 0.49 g L^{-1}). After 96 h of fermentation, CGXII with 50 g per L sugar yielded 0.31 ± 0.01 g per L putrescine (Fig. 2a). The increased concentration of glucose of 60 g L^{-1} and above could not drastically improve either the putrescine or the 5AVA titer which may be due to the increased metabolic burden that results from excessive glycolytic flux.[3,26] Therefore, maintaining the glucose concentration is crucial for the optimal production of both 5AVA and putrescine.

3.1.2. Effect of ammonium sulphate concentration. Ammonium sulphate acts as the primary nitrogen donor for the biosynthesis of two amino acid precursors ornithine and lysine and its conversion to putrescine and 5AVA is also nitrogen dependent.[27] It was observed that 3.13 ± 0.09 g L^{-1} of 5AVA was produced after 120 h of fermentation when 30 g L^{-1} of ammonium sulphate was used and interestingly when 40 g L^{-1} was used, it gave almost the same 5AVA titer of 3.1 ± 0.36 g L^{-1} (Fig. 1b). This study demonstrated that for further experiments, the concentration of ammonium sulphate can be reduced to 30 g L^{-1} in the case of 5AVA. It was also observed that a maximum putrescine titer of 0.36 ± 0.01 g L^{-1} was obtained after 96 h of fermentation where the initial ammonium sulphate level was 20 g L^{-1} (Fig. 2b) and it showed a decrease when the concentration increased to 25 g L^{-1}.

3.1.3. Effect of MOPS. After 120 h of fermentation, 3.07 ± 0.12 g L^{-1} of 5AVA was obtained when the control concentration of MOPS (40g L^{-1}) was used and a maximum 5AVA titer of 4.11 ± 0.52 g L^{-1} was obtained after 96 h when the initial MOPS was decreased to 30 g L^{-1}. Further reduction in MOPS to 20 g L^{-1} yielded 3.93 ± 0.16 g L^{-1} but a reduction of MOPS to 10 g L^{-1} declined the 5AVA titer to 3.23 ± 0.87 g L^{-1} (Fig. 1c). Similarly, a putrescine titer of 0.30 ± 0.01 g L^{-1} was obtained after 96 h of fermentation, when 40 g per L MOPS was used which was improved to 0.45 ± 0.01 g L^{-1} when the initial concentration of MOPS was set to 20 g L^{-1} (Fig. 2c). Thus, in both the cases it was observed that reducing the MOPS concentration up to 20 g L^{-1}

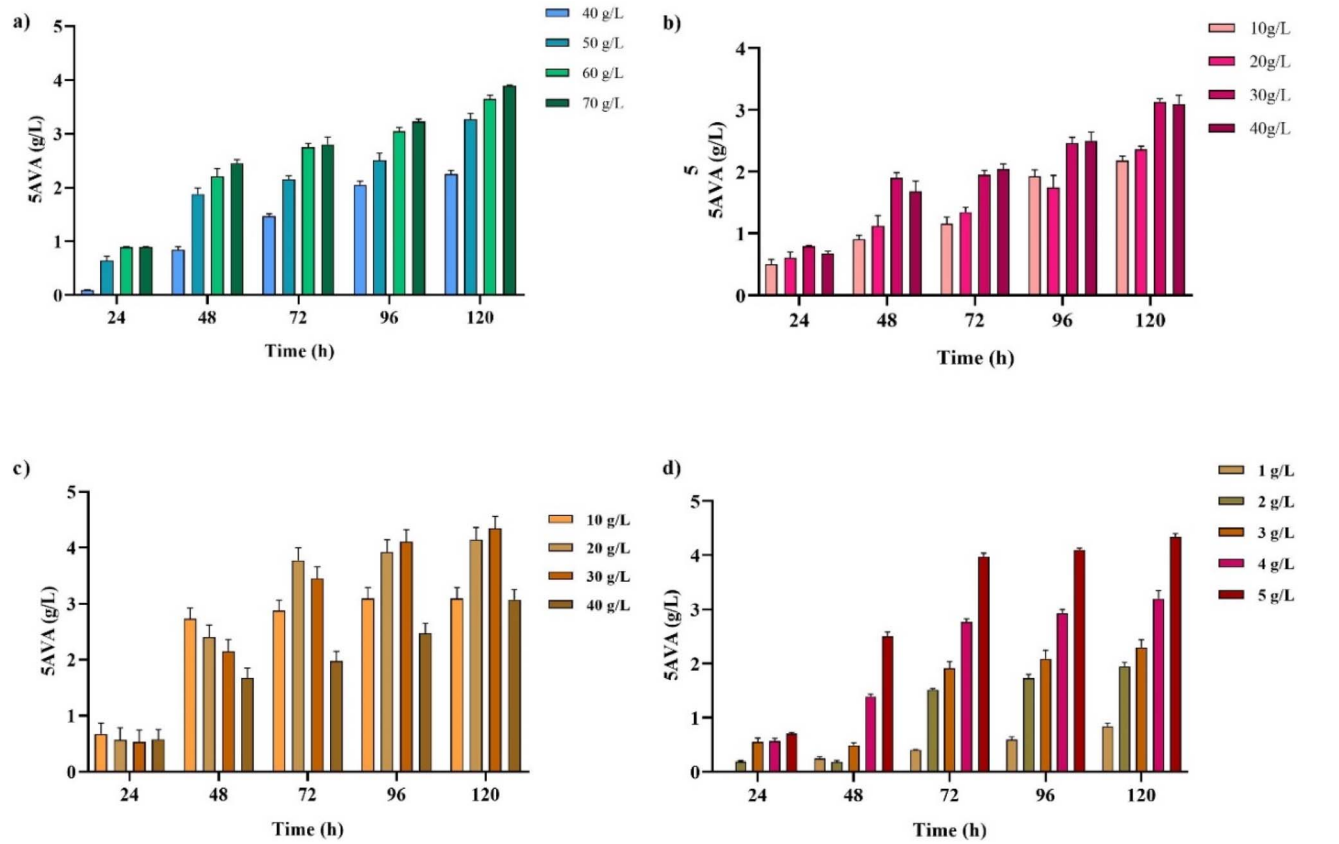

Fig. 1 Optimization of medium components in CGXII medium for 5AVA production: (a) glucose (40–70 g L^{-1}), (b) ammonium sulphate (10–40 g L^{-1}), (c) MOPS (10–40 g L^{-1}) and (d) urea (1–5 g L^{-1}).

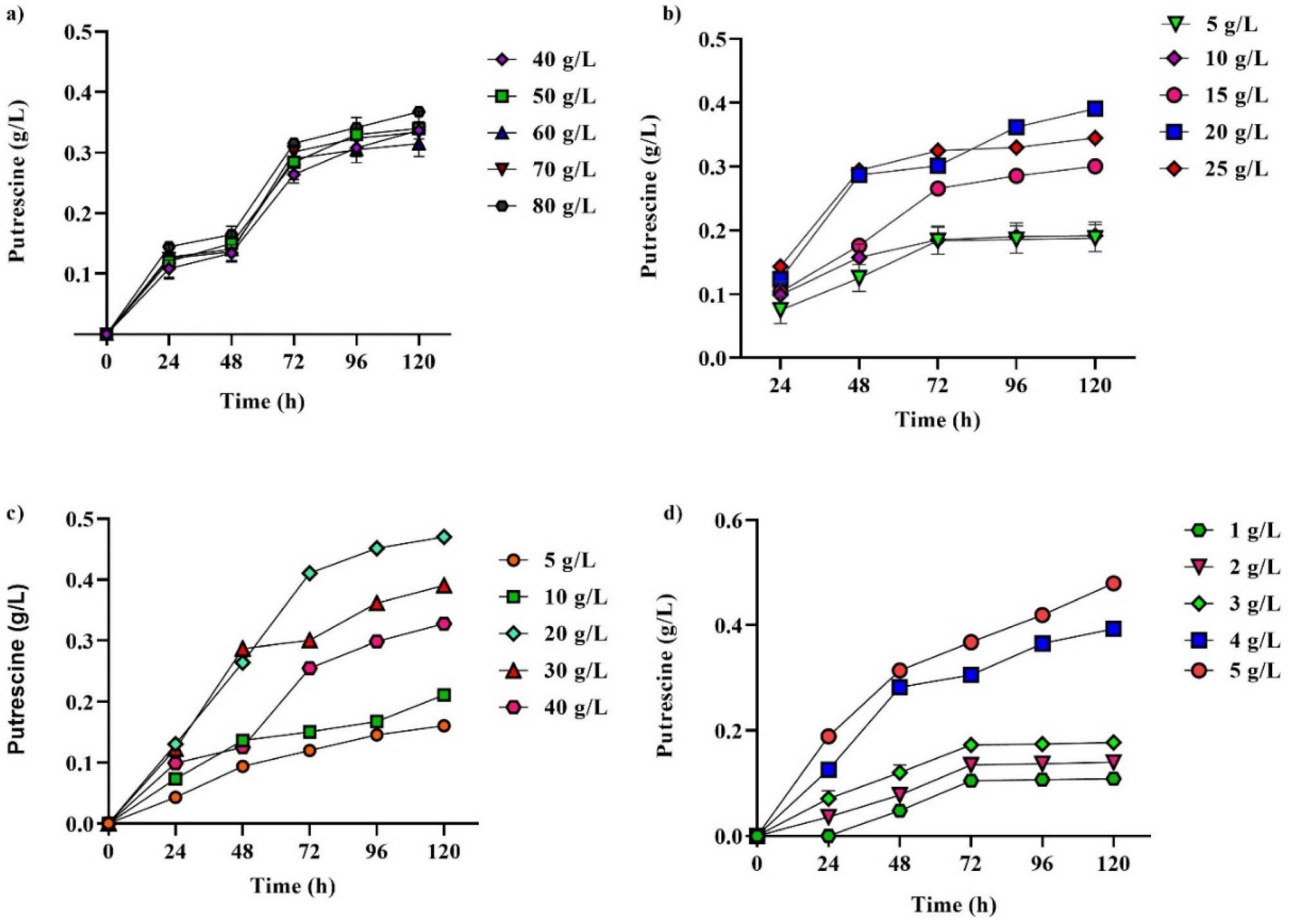

Fig. 2 Optimization of medium components in CGXII synthetic medium for putrescine production: (a) concentration of glucose (40–80 g L^{-1}), (b) ammonium sulphate (5–25 g L^{-1}), (c) MOPS (5–40 g L^{-1}) and (d) urea (1–5 g L^{-1}).

did not affect the production titer. Variations in the concentration of ammonium salts might fluctuate the pH which might in turn demand more MOPS for the buffering. MOPS being an organic buffer plays a key role in stabilizing the pH of the CGXII medium and maintaining optimum conditions of the intracellular enzyme system for the biosynthesis of these molecules. During the optimization of MOPS, pH was checked at the start and end of the runs. Across the range of MOPS concentrations tested, in cases of 5-AVA and putrescine, final pH values remained within pH 6.8 to 7.0, indicating that MOPS acted to stabilize the medium rather than to alter its intrinsic pH. On the other hand, an excessive concentration of MOPS may disrupt the ion balance of the cell, in turn affecting the metabolic flux. MOPS is a relatively expensive buffering agent in the fermentation medium; reducing its concentration offers a promising approach to enhance the cost-effectiveness of the process without compromising the overall system performance. While MOPS is appropriate for laboratory scale studies to maintain pH stability, it would be replaced by more economical buffering strategies at the industrial scale to reduce production costs.

3.1.4. Effect of urea concentration. Urea being a slow nitrogen releaser is used in the CGXII medium along with ammonium sulphate as a nitrogen source.[27] Among the concentrations of urea tested, 5 g L^{-1} of urea in CGXII gave a 5AVA titer of 4.1 ± 0.2 g L^{-1} (Fig. 1d) and putrescine of 0.41 ± 0.01 g L^{-1} after 96 h of fermentation (Fig. 2d). In both cases, the production tended to decline when the concentration of urea was decreased and a further increase in urea didn't favour the product titer. Later, through successive sub-culturing of PUT Xyl and fermentation, the putrescine titer was improved to 1.82 ± 0.39 g L^{-1} (data not shown).

3.2. Central composite design (CCD) for optimization of medium components for 5AVA production by *C. glutamicum* AVA Xyl

The optimum levels of key medium components (ammonium sulphate, MOPS, glucose and xylose) and the interactions between the variables were interpreted using a central composite design (CCD).[28] The design matrix of the CCD design experiment for 5AVA production as shown in Table 1 comprised three levels – low (−1), medium (0), and high (+1). A quadratic eqn (2) was obtained by the analysis of data, using Minitab 17 software, in which the response is the 5AVA titer (Y) expressed as a function of test variables X_1, X_2, X_3 and X_4 where they represent ammonium sulphate, MOPS, glucose and xylose.

Table 1 Design matrix and test results of CCD for 5AVA production

Run order	Ammonium sulphate (g L^{-1})	MOPS (g L^{-1})	Glucose (g L^{-1})	Xylose (g L^{-1})	5AVA (g L^{-1})
1	20	30	30	10	5.00
2	10	30	10	10	2.30
3	15	15	20	20	3.00
4	15	25	20	40	4.67
5	15	25	20	20	5.70
6	10	20	30	10	3.60
7	20	30	30	30	5.90
8	20	20	10	10	2.80
9	20	20	10	30	4.30
10	10	30	30	30	4.50
11	15	25	20	20	5.50
12	10	20	30	30	3.30
13	15	35	20	20	4.00
14	20	30	10	10	2.50
15	10	30	10	30	2.80
16	15	25	20	20	5.60
17	10	30	30	10	4.50
18	5	25	20	20	2.40
19	**15**	**25**	**20**	**20**	**6.00**
20	15	25	20	20	6.00
21	20	20	30	30	5.80
22	10	20	10	10	2.30
23	15	25	20	0	3.20
24	15	25	20	20	5.50
25	20	30	10	30	3.80
26	15	25	40	20	5.40
27	20	20	30	10	4.30
28	25	25	20	20	4.50
29	10	20	10	30	2.50
30	15	25	0	20	1.88
31	15	25	20	20	6.00

$$Y = -19.71 + 0.7626X_1 + 1.1315X_2 + 0.1702X_3 + 0.1428X_4 - 0.02220X_1 \times X_1 - 0.02170{X_2}^2 - 0.005074{X_3}^2 - 0.004337{X_4}^2 - 0.00600X_1 \times X_2 + 0.00200X_1 \times X_3 + 0.00600X_1 \times X_4 + 0.00425X_2 \times X_3 - 0.00025X_2 \times X_4 - 0.000875X_3 \times X_4 \quad (2)$$

The highest 5AVA titer of 6.00 ± 0.54 g L^{-1} was achieved in run number 19 using a combination of 15 g per L ammonium sulphate, 25 g per L MOPS, 20 g per L glucose and 20 g per L xylose. The interrelation of the medium components and the fitted response for the above regression model is pictured as surface plots in Fig. 3, where the 5AVA titer is the response. The surface plot (Fig. 3a) shows an increasing trend of AVA as the concentrations of glucose and xylose increase but there is a saturation point where a further increase does not boost the 5AVA titer. The highest 5AVA values are observed in the upper right region of the plot, where glucose (~45 g L^{-1}) and xylose (~30 g L^{-1}) are relatively high. The plot (Fig. 3b) suggests that both MOPS and xylose contribute positively to 5AVA production, *i.e.*, where about 6 g L^{-1} of 5AVA accumulated when the MOPS is around 24 to 30 g L^{-1} and xylose is 30–45 g L^{-1}. The influence of ammonium sulphate and xylose on the 5AVA titer is depicted in Fig. 3c. Here also, both factors positively contribute to 5AVA production.

The curve illustrating the effect of MOPS and glucose on 5AVA (Fig. 3d) similarly suggests a non-linear relationship. Fig. 3e (interaction between ammonium sulphate and MOPS) and Fig. 3f (ammonium sulphate and glucose) also show a similar pattern. Under all the conditions, a saturation effect exists rather than a continuous increase in 5AVA with higher concentrations of the variables. These non-linear relationships indicate that while higher levels of factors enhance 5AVA production, their impact decreases at excessive concentrations, suggesting limited response beyond a certain threshold. The response surface plots illustrate the interactive effects of key nutrients, highlighting the influence of ammonium sulphate, MOPS, glucose, and xylose.

Although increased concentrations generally promote production, excessive levels may lead to metabolic saturation and feedback inhibition.[29] Thus, a multifactorial statistical approach that accounts for the interactions among independent variables serves as a foundation for modelling the nonlinear nature of the response in short-term experiments.[30–33] Further experimental validation is needed to refine these findings and develop large-scale bioproduction strategies.

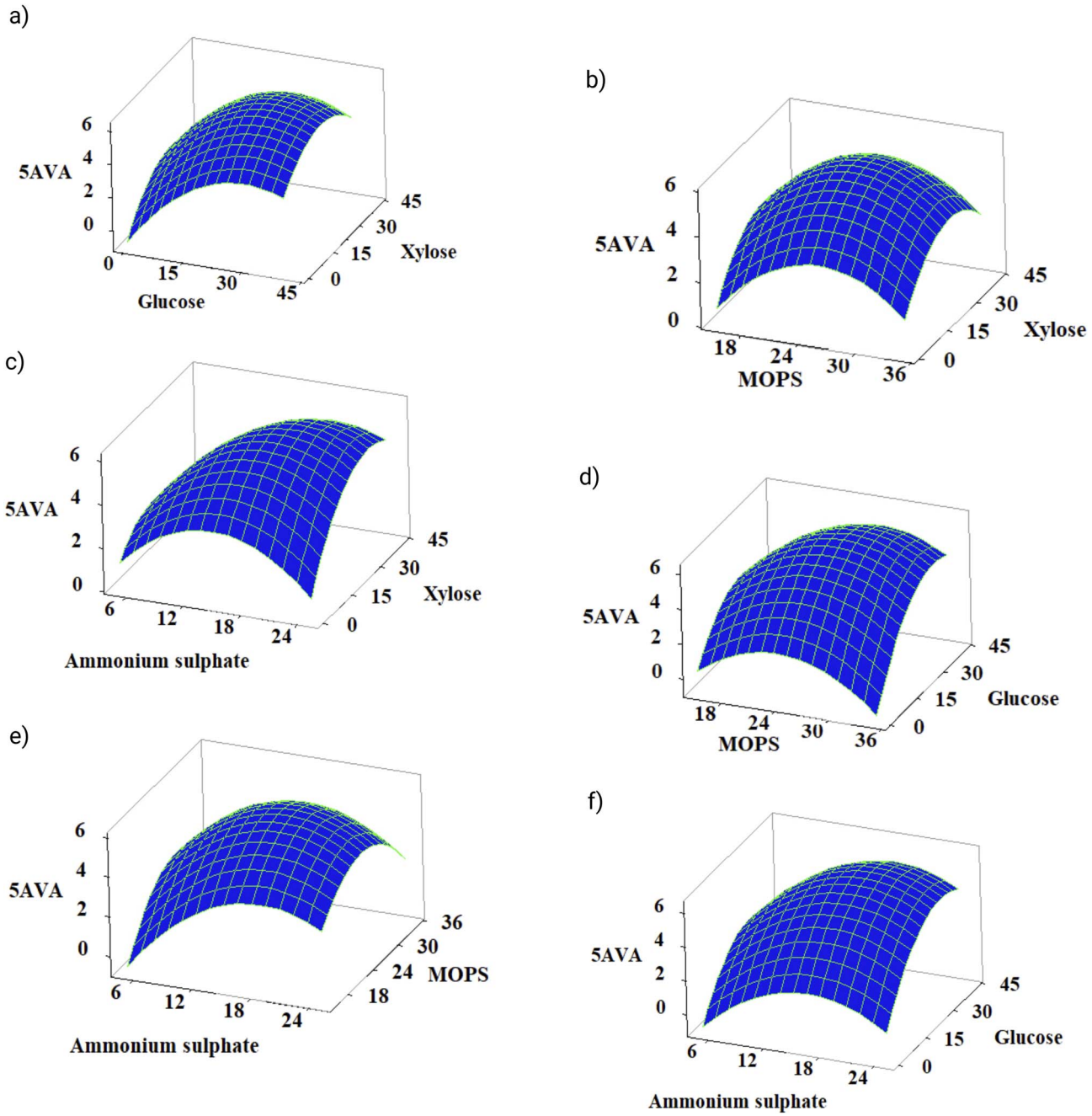

Fig. 3 Surface plots of the interaction of the medium components: ammonium sulphate, MOPS, glucose and xylose on 5AVA production by *C. glutamicum* AVA Xyl. Interactions include the synergy of (a) glucose and xylose (b) MOPS and xylose (c) ammonium sulphate and xylose (d) MOPS and glucose (e) ammonium sulphate and MOPS (f) ammonium sulphate and glucose.

3.3. Design matrix and test results of CCD for putrescine production

The variable value ranges were set according to the results obtained from the OFAT experiments and the CCD design experiment ($N = 32$) was conducted, where the matrix comprised three levels – low (-1), medium (0), and high ($+1$) as shown in Table 2. A second-order polynomial eqn (3) was obtained by the analysis of data, using the Minitab 17 software, in which the response is the putrescine titer (Y) expressed as a function of test variables X_1, X_2, X_3, X_4 and X_5 where they represent glucose, xylose, ammonium sulphate, MOPS and urea respectively.

$$\begin{aligned} Y = {} & -15.02 + 1.3149X_1 + 0.5845X_2 + 2.858X_3 \\ & - 0.2052X_4 + 0.2092X_5 - 0.02258{X_1}^2 - 0.00958{X_2}^2 \\ & - 0.0850{X_3}^2 + 0.001949{X_4}^2 - 0.003058{X_5}^2 \\ & - 0.01387X_1 \times X_2 + 0.00277X_1 \times X_3 - 0.00398X_1 \\ & \times X_4 - 0.00817X_1 \times X_5 - 0.08011X_2 \times X_3 \\ & + 0.00775X_2 \times X_4 + 0.00353X_2 \times X_5 - 0.00219X_3 \\ & \times X_4 + 0.00209X_3 \times X_5 - 0.002403X_4 \times X_5 \end{aligned} \quad (3)$$

Table 2 Central composite design for optimization of medium components putrescine production by *C. glutamicum* PUT Xyl

Run order	Ammonium sulphate (g L^{-1})	MOPS (g L^{-1})	Urea (g L^{-1})	Glucose (g L^{-1})	Xylose (g L^{-1})	Putrescine (g L^{-1})
1	15	25	3.5	30	40	4.10
2	15	25	3.5	30	20	5.15
3	20	30	2	20	30	3.69
4	15	25	0.5	30	20	3.80
5	10	30	5	20	30	4.40
6	15	25	3.5	10	20	6.44
7	10	20	5	40	30	4.88
8	10	30	2	20	10	3.42
9	15	25	3.5	30	20	5.43
10	15	35	3.5	30	20	3.58
11	20	20	2	20	10	5.31
12	20	30	2	40	10	4.68
13	25	25	3.5	30	20	3.61
14	15	25	3.5	30	20	5.78
15	10	20	2	20	30	3.97
16	15	25	3.5	30	20	5.51
17	10	30	5	40	10	4.31
18	**20**	**20**	**5**	**20**	**30**	**6.44**
19	10	30	2	40	30	5.27
20	15	15	3.5	30	20	5.56
21	15	25	3.5	30	0	4.51
22	10	20	5	20	10	5.29
23	15	25	3.5	50	20	6.17
24	20	30	5	20	10	3.60
25	20	20	2	40	30	2.48
26	15	25	3.5	30	20	5.60
27	20	20	5	40	10	6.34
28	10	20	2	40	10	3.29
29	20	30	5	40	30	3.02
30	15	25	3.5	30	20	5.57
31	15	25	6.5	30	20	5.72
32	5	25	3.5	30	20	2.92

A maximum putrescine titer of 6.44 ± 0.33 g L^{-1} was obtained in run number 18 from a combination of 20 g per L ammonium sulphate, 20 g per L MOPS, 5 g per L urea, 20 g per L glucose and 30 g per L xylose. The contour maps that represent the interaction between the variables, where putrescine titer was obtained as the response, are presented in Fig. 4. The interaction of MOPS, urea, glucose and xylose with the ammonium sulphate concentration is depicted in Fig. 4a–d. The increase in the MOPS concentration up to 25 g L^{-1} (Fig. 4a) enhances the putrescine titer to 5.5 g L^{-1} and then decreases with a further increase in ammonium sulphate. At this stage, urea (3.5 g L^{-1}), glucose (30 g L^{-1}) and xylose (20 g L^{-1}) were constant. Similarly, as depicted in Fig. 4b, the urea concentration above 3.5 g L^{-1} increases putrescine to 5.75 g L^{-1}, where MOPS (5 g L^{-1}), glucose (30 g L^{-1}) and xylose (20 g L^{-1}) were at constant levels. Fig. 4c shows the synergy of ammonium sulphate and glucose where ammonium sulphate above 7 g L^{-1} accumulates putrescine in the range of 4–6 g L^{-1} irrespective of the increase in the glucose concentration but the highest titer of putrescine (>6 g L^{-1}) was observed within 10–16 g L^{-1} of glucose. Here, the hold values of MOPS, urea and xylose were 25 g L^{-1}, 3.5 g L^{-1} and 20 g L^{-1} respectively. In the case of xylose and ammonium sulphate, a xylose concentration of 4–27 g L^{-1} gave maximum putrescine (>5.1) when ammonium sulphate was between 12.5 and 21 g L^{-1} (Fig. 4d). Glucose and xylose showed a non-linear influence on putrescine. The highest putrescine concentrations (>6.44 g L^{-1}) occur in regions where both glucose and xylose at moderate levels where ammonium sulphate (15 g L^{-1}), MOPS (25 g L^{-1}) and urea (3.5 g L^{-1}) are constant (Fig. 4e). The synergy of MOPS with glucose is portrayed in Fig. 4f, where higher glucose (50 g L^{-1}) and moderate MOPS (15–20 g L^{-1}) favoured higher putrescine production (>7 g L^{-1}). In the case of xylose and MOPS (Fig. 4g), optimal putrescine production (>5.5 g L^{-1}) occurs when xylose is around 10–20 g L^{-1} and MOPS are around 20–25 g L^{-1}. High xylose or very low/high MOPS reduces putrescine production. The confluence of urea and MOPS (Fig. 4h) depicted that 5–6 g L^{-1} of urea results in the highest putrescine production (>6.5 g L^{-1}) which implies that urea is essential for putrescine production. The lowest putrescine levels (<2 g L^{-1}) occur when urea and MOPS are very low, suggesting a synergistic effect between the two factors. As shown in Fig. 4i, the maximum putrescine production occurs when both glucose (50 g L^{-1}) and urea (5–6 g L^{-1}) are at higher levels. Lower levels of either factor reduce putrescine production; thus, a balance between glucose and urea is crucial. The contour of putrescine *vs.* xylose and urea is shown in Fig. 4j, where 4 g L^{-1} of urea is optimal for putrescine production. Putrescine levels remain relatively stable across different xylose concentrations with

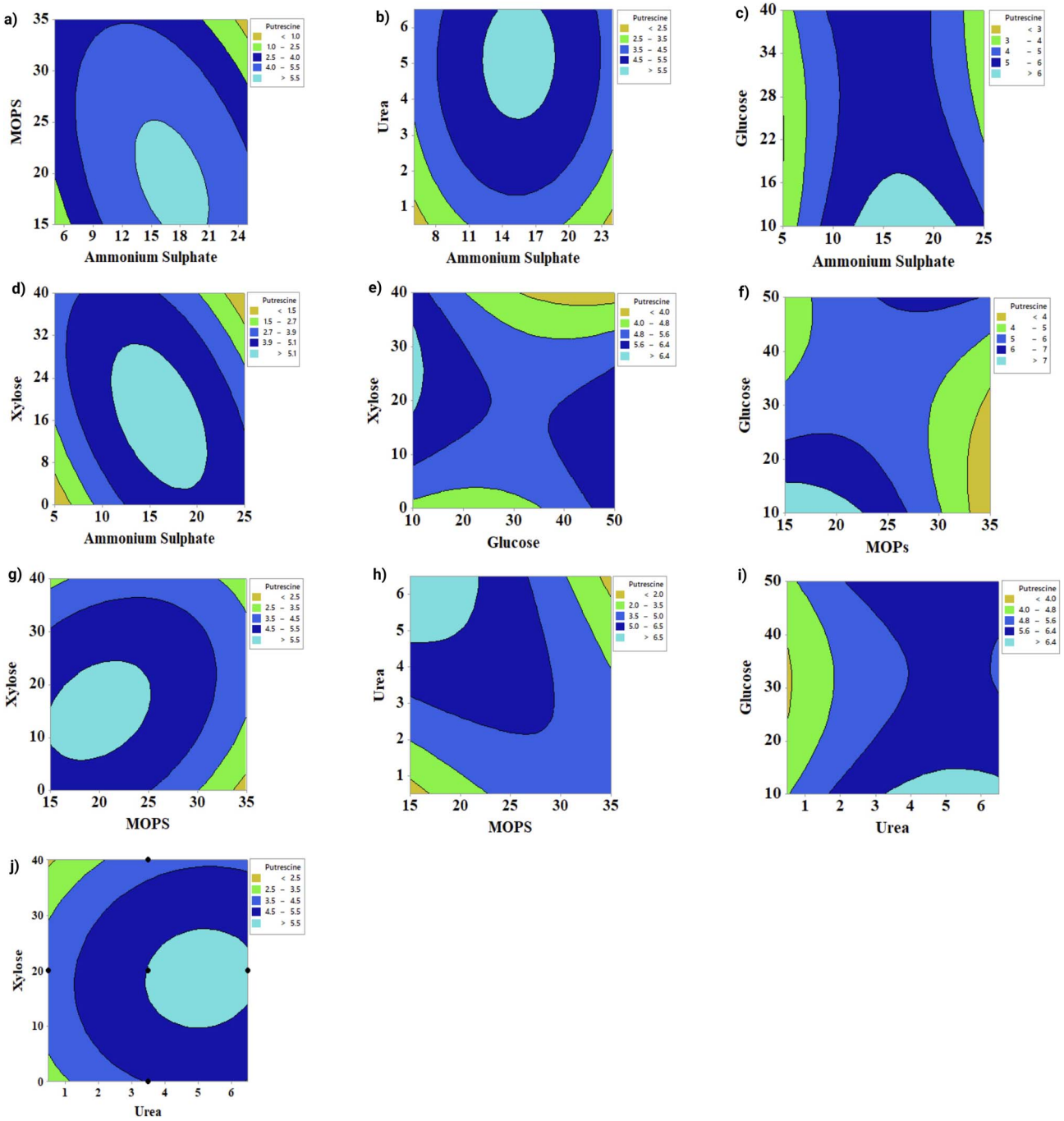

Fig. 4 Contour plots depicting the interaction of medium components in putrescine production by *C. glutamicum* PUT Xyl. Interactions include the synergy of (a) ammonium sulphate and MOPS, (b) ammonium sulphate and urea, (c) ammonium sulphate and glucose, (d) ammonium sulphate and xylose, (e) glucose and xylose, (f) MOPS and glucose, (g) MOPS and xylose, (h) urea and xylose (i) urea and glucose and (j) urea and xylose. The hold values indicate the factors at constant concentrations.

the highest (>5.5 g L^{-1}) being in between 20 and 30 g L^{-1} of xylose, indicating a positive influence of xylose on putrescine production.

3.4. The variance analysis and significance of the 5AVA and putrescine experimental model by ANOVA

The experimental model for the production of putrescine and 5AVA was analysed by ANOVA and the significance of the model was evaluated using the probability value (*p*-value). As given in Tables S1 and S2, a lower probability value ($p < 0.05$) indicated that the model was significant in both cases. The ANOVA (Table S1) for the variance analysis of 5AVA revealed that the linear terms have a strong influence on the response and glucose is the most influential factor (*F*-value 93.97) among the linear terms. Among the quadratic terms, ammonium sulphate, MOPS and glucose with high *F*-values possessed the most pronounced effect. In the combinatorial effect, the interaction

of MOPS × xylose ($p = 0.808$) and glucose × xylose ($p = 0.103$) is non-significant. The interrelations of ammonium sulphate × MOPS ($p < 0.05$), ammonium sulphate × xylose ($p < 0.05$) and MOPS × glucose ($p < 0.05$) are the most impactful interactions. The lack of fit (F-value = 0.57) test is non-significant affirming that the model adequately fits the data.

In the case of putrescine production, the model F-value is 43.66 and $p < 0.001$, which denotes that the overall model is highly significant. All the linear components of the factors are significant and the linear terms have a significant F-value (39.41). The individual quadratic terms of all the factors exhibit significant ($p < 0.05$) non-linear effects, particularly for ammonium sulphate, MOPS, urea and glucose. The most influential ($p > 0.05$) two-way interactions include ammonium sulphate × MOPS, ammonium sulphate × glucose, MOPS × urea, MOPS × glucose, and glucose × xylose whereas the interactions of ammonium sulphate × urea, urea × glucose, and urea × xylose are not statistically significant ($p > 0.05$). The lack-of-fit F-value (1.01) suggested that there is no significant lack of fit and deduced that the model fits the data well. The results of the variance analysis of the regression model for putrescine are given in Table S2.

3.5. Validation experiment

The results of the validation experiments are tabulated in Table 3. The experimental and predicted values for the response of validation experiments of 5AVA and putrescine were highly correlated and it reflects the accuracy of the model.

3.6. Extraction and purification of the nylon monomers from the fermented broth

3.6.1. 5AVA recovery. The schematic principle of 5AVA adsorption onto Dowex 50W-X8 resin is shown in Fig. 5a and it is found that irrespective of the initial load given the adsorption percentage was around 96% (Fig. 5b). 5AVA is a zwitter ionic compound. The strongest acidic and strongest basic pK_a values of 5AVA are 4.65 and 10.21 respectively. An optimum pH is essential for ideal adsorption, wherein a wide pH range from 2–8 was checked to determine the suitable pH. At low pH (2–4), the adsorption capacity was found to be the highest (5.8–6 mg g^{-1}) as shown in Fig. 5c. This may be due to the conversion of 5AVA to its protonated ($-NH_3^+$) form that enhances its electrostatic attraction to the cation exchange resin. At pH 5–8, a reduction in the adsorption is observed indicating a decline in the electrostatic interaction which might be due to deprotonation of 5AVA, making it less interactive with the adsorbent surface. Accordingly, by balancing the charge availability and operational efficiency mitigating microbial contamination concerns, pH 4–5 was found to be ideal. Subsequently, the contact time was optimised to 50 minutes as shown in Fig. 5d. For efficient elution, 1 N NaOH was used and 84 ± 2% of 5AVA was desorbed efficiently.

The resin operates on the principle of cation exchange and the method employed leverages the cationic nature of 5AVA at low pH for efficient binding to a cation exchange resin, followed by selective elution with sodium hydroxide. 5AVA was adsorbed at pH 4.5 on Dowex 50W-X8 resins and effectually eluted by 1 N NaOH after a contact time of 30 minutes. The recovery efficiency of 5AVA was 84 ± 2%. The high pH of NH_4OH disrupts the ionic interactions between the cationic 5AVA and the resin, facilitating the release of the bound compound. The HPLC chromatogram (Fig. 5e) reveals the purity of the recovered 5AVA. This method of elution is found to be both efficient and selective, minimizing co-elution of non-target impurities.

The resin was reused for five consecutive cycles, with regeneration between each run. As shown in Fig. 5f, recovery yields remained at 77.5 ± 1.78% for the first four cycles, but declined more markedly by the fifth cycle. These results indicate that the resin can be reused for at least four cycles with acceptable recovery efficiency.

3.6.2. Putrescine recovery. After the clarification with activated charcoal treatment, the filtered cell-free fermented broth was acidified to a pH of 4.5 to protonate the amino groups of

Table 3 The model predicted and experimental values of 5AVA and putrescine titer

				5AVA (g L^{-1})	
Ammonium sulphate (g L^{-1})	MOPS (g L^{-1})	Glucose (g L^{-1})	Xylose (g L^{-1})	Actual	Predicted
20	30	30	30	5.90	6.01
10	30	30	30	4.50	4.45
15	35	20	20	4.00	3.95
15	25	20	20	6.00	5.76
25	25	20	20	4.50	4.60

					Putrescine (g L^{-1})	
Ammonium sulphate (g L^{-1})	MOPS (g L^{-1})	Glucose (g L^{-1})	Xylose (g L^{-1})	Urea (g L^{-1})	Actual	Predicted
15	25	10	20	3.5	6.44	6.49
15	35	30	20	3.5	3.58	3.75
20	30	40	10	2	4.68	4.66
10	20	20	10	5	5.29	5.30
15	25	30	20	3.5	5.60	5.51

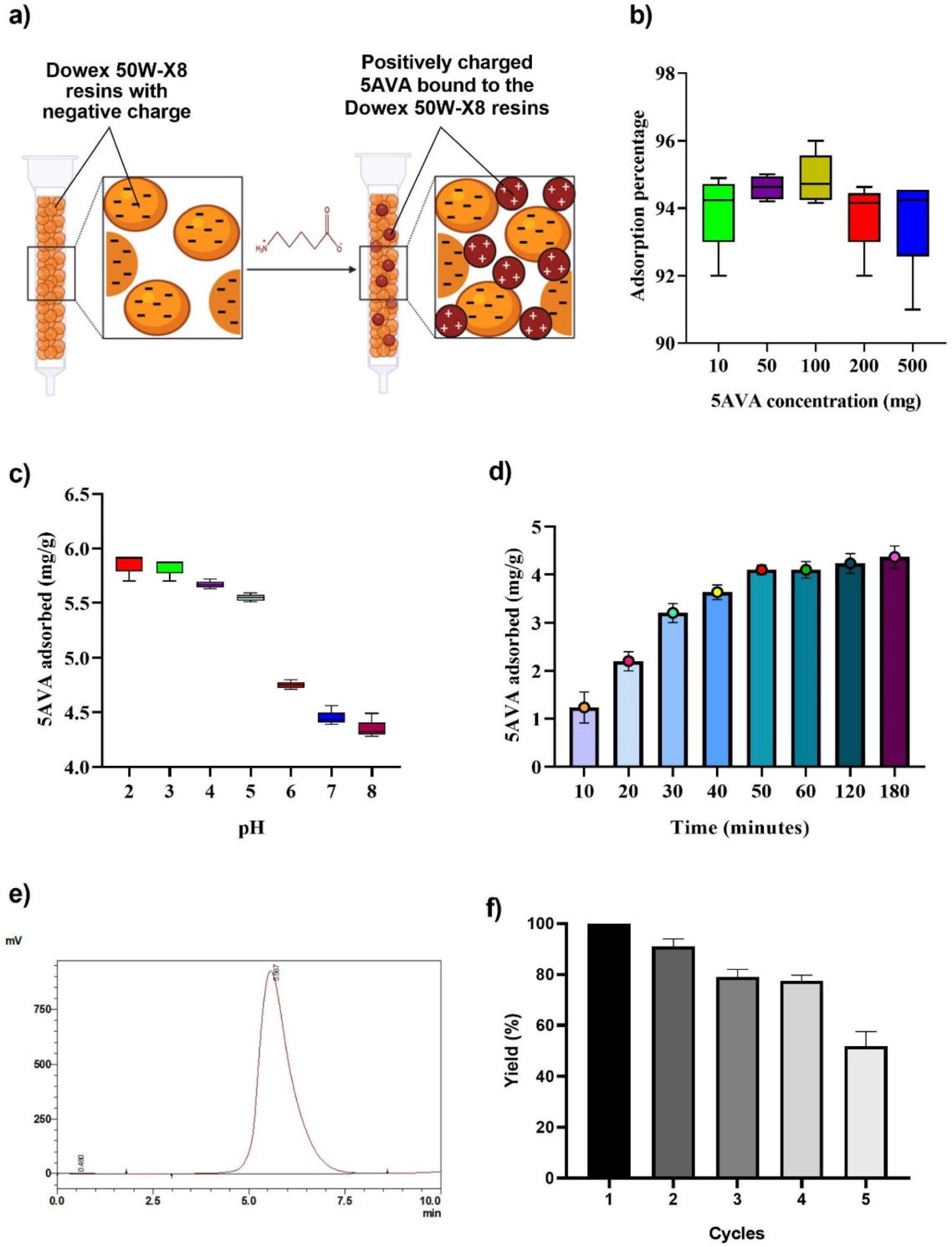

Fig. 5 Recovery of 5AVA from fermented broth. (a) Schematic representation of 5AVA adsorption onto Dowex 50W-X8 resin, (b) adsorption capacity of the resin, (c) effect of pH, (d) effect of contact time for the ion exchange chromatography using Dowex 50W-X8 resin for the recovery of 5AVA (e) HPLC chromatogram of purified 5AVA and (f) reusability of the resin.

putrescine thereby increasing the solubility of putrescine in the aqueous phase. A subsequent centrifugation was done to remove the precipitated residual proteins, if any. The broth was then alkalinized to a near-neutral pH of 6–6.5 and a series of controlled evaporations were performed to concentrate putrescine from the broth.[25] The initial mild evaporation at 35–40 °C and 340 mbar pressure for 12 h incrementally removed the bulk water content reducing the broth volume by almost 65 $\pm$ 3% and concentrated putrescine to 11.2 $\pm$ 0.87 g L^{-1} (Fig. 6a). The low-temperature vacuum evaporation prevents the

volatilization of putrescine. Furthermore, the residual water and low boiling point impurities were separated by controlled evaporation at a slightly higher temperature of 50–55 °C but a 340 mbar pressure did not further remove the water content. Therefore, the pressure was further decreased and optimised for the last step.

The final evaporation at 65–70 °C and 20 mbar effectively removed residual water, increasing the putrescine concentration to 14.32 ± 0.61 g L^{-1} (Fig. 6b and c). The controlled escalation of temperature and pressure ensured that putrescine was not exposed to harsh conditions. The pH correction significantly improved the yield and purity of putrescine as a lower recovery rate was observed when the step-wise evaporation was done without the pH adjustment. The HPLC analysis of the purity and yield of purified and crude putrescine (Fig. 6d) exhibited a 2.3-fold increase in the putrescine concentration demonstrating the sequential evaporation process to be efficient for the recovery of putrescine. The FTIR spectra of purified putrescine and the standard (Fig. 6e) displayed characteristic absorption bands, including N–H stretching at 3300–3400 cm^{-1}, methylene C–H stretching at 2850–2950 cm^{-1}, N–H bending at around 1600 cm^{-1}, and C–N stretching within 1000–1200 cm^{-1},[34,35] confirming purification, with minor band broadening likely due to residual moisture or trace impurities.

In our earlier study,[5] we reported that *C. glutamicum* strains AVA Xyl and PUT Xyl exhibited limited growth when cultivated on xylose as the sole carbon source, indicating that xylose alone was insufficient to support the biomass accumulation required for efficient production. Based on these findings, xylose was deliberately excluded as a variable in our initial one-factor-at-a-time (OFAT) optimization, where the focus was on establishing a robust growth profile using glucose as the primary carbon source. However, since the strain contains a plasmid-based system for xylose utilization, we hypothesized that the interaction between glucose and xylose could play a critical role not only in maintaining cell viability but also in enhancing pathway expression and such interactions were explored using CCD. The synergistic impact of carbon source interaction, which could not have been captured through single-variable screening, underscores the necessity of multifactorial designs in strain-process integration, especially when plasmid-based expression systems are employed. The putrescine titer is at par and a little ahead of the previous report on *C. glutamicum*.[36] Earlier studies have reported titres 3.6 g L^{-1} of 5AVA[1] and 1.68 g L^{-1} of putrescine,[37] using metabolically engineered *E. coli* strains. The

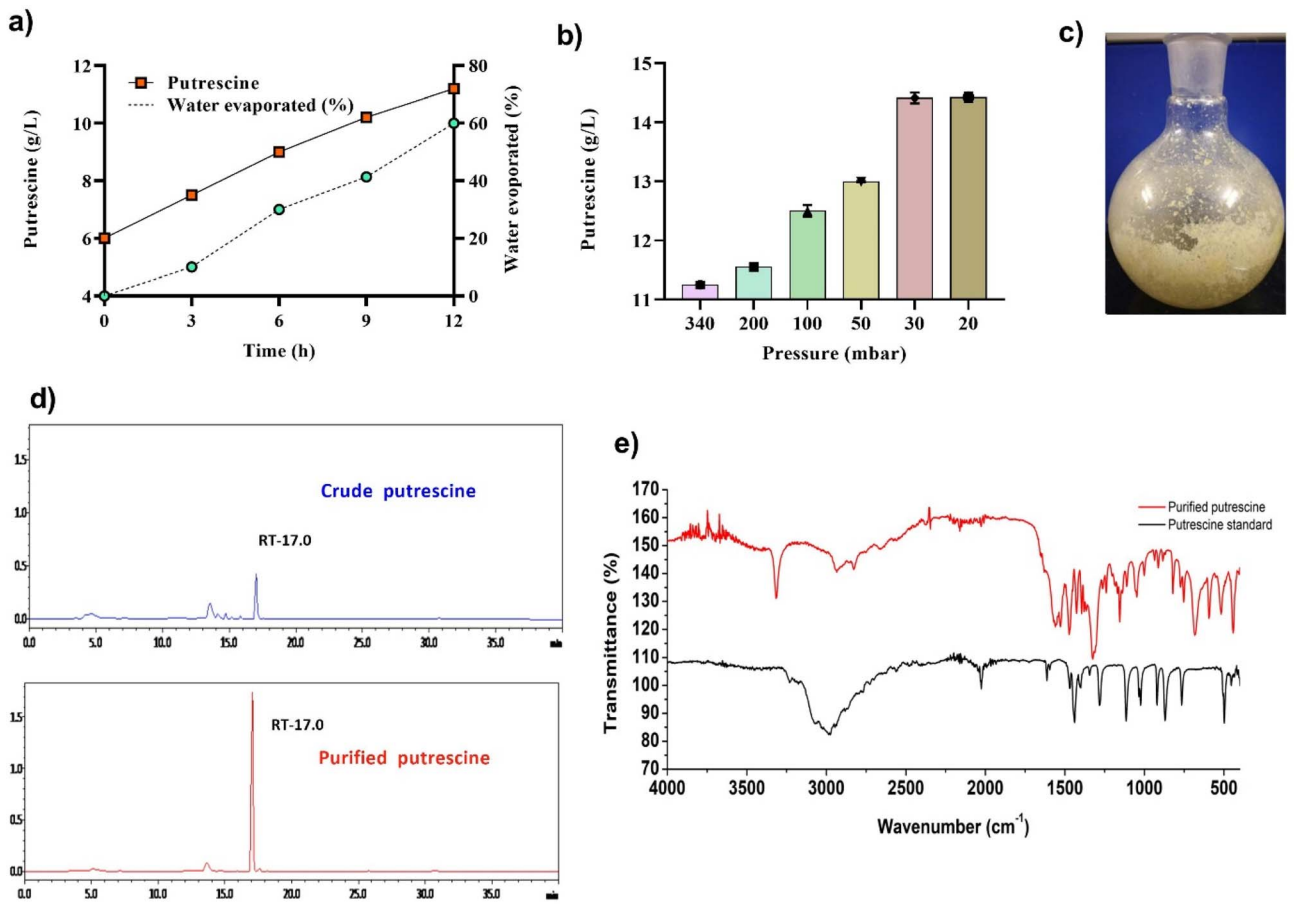

Fig. 6 Recovery of putrescine from fermented broth. (a) Initial evaporation and concentration of putrescine, (b) final evaporation and concentration of putrescine, (c) concentrated putrescine in the round bottom flask after final refining and (d) HPLC chromatogram of crude putrescine at RT-17.0 and the HPLC chromatogram of concentrated putrescine after purification (RT-17.0). (e) FTIR spectrum of purified putrescine and standard putrescine. Abbreviation: RT, retention time.

significant increase in putrescine titre from 1.82 ± 0.39 g L^{-1} to 6.44 g L^{-1} demonstrates the critical impact of platform-wide parameter interaction, rather than isolated variable tuning, providing mechanistic reasoning. Similarly, the AVA titre of 6.0 ± 0.54 g L^{-1} is ahead of other reports by batch fermentation. Previous reports of titers and yields of 5-aminovaleric acid (5-AVA) and putrescine obtained using different microbial hosts and feedstocks are summarised in Table S3. The metabolically engineered strains used also helped to minimize by-product formation, offering a significant advantage in terms of purification and sustainability. The rationale behind our separation strategies also reflects green chemistry principles: AVA, being polar and less volatile, was efficiently recovered through ion-exchange chromatography using Dowex 50W-X8 resin (yield: 84 ± 2%), while putrescine, due to its lower polarity and moderate volatility, was more effectively concentrated *via* vacuum assisted evaporation (up to 14.3 ± 0.6 g L^{-1}). Chromatographic methods were found to be economically and operationally suboptimal for putrescine due to its weak interaction with resins. These compound-specific downstream approaches reduce solvent use and energy intensity, aligning the process with principles of green separation.

3.6.2.1 Preliminary techno-economic considerations. To provide an economic perspective on our process, we performed a simplified technoeconomic assessment (TEA) focused on feedstock and downstream operating costs. From the best runs, 6.0 g per L 5-AVA was produced from 20 g per L glucose and 20 g per L xylose with a yield of 0.15 g g^{-1} sugar and 6.44 g L^{-1} of putrescine from 20 g per L glucose and 30 g per L xylose with a yield of 0.13 g g^{-1} sugar. Using the measured best run compositions, we estimate the sugar requirement per kg product to be ∼6.7 kg and ∼7.8 kg for 5-AVA and putrescine, respectively. In this work, the experiments were performed with reagent-grade glucose and xylose (HiMedia). However, these prices reflect analytical-grade chemicals and are not representative of industrial feedstock supply. Using such values would imply high feedstock costs, which is unrealistic for scale-up. For TEA purposes we therefore adopt commodity-scale lignocellulosic sugar prices, which better reflect potential industrial scenarios. Assuming conservative bulk sugar costs of USD 0.20–0.50 per kg, the feedstock contribution corresponds to ∼USD 2–3 per kg product. This range is consistent with values reported in the literature: for first-generation crops, sugar production costs typically range from USD 0.22–0.55 per kg, while for cellulosic crops costs can span USD 0.10–3.37 per kg sugar, depending on pretreatment and conversion efficiency.[38] Overall, the analysis indicates that current yields and titers remain below typical commodity targets.[39] Yield and titer improvements thus represent the strongest levers to reduce costs. Nevertheless, co-utilization of xylose, an abundant and relatively underutilized fraction of lignocellulosic hydrolysates, combined with low-solvent downstream processing, provides a promising route to improve both the economic and environmental performance of putrescine and 5-AVA production. The novelty of this work lies primarily in the statistical optimization of medium components and the demonstration of effective downstream processing for recovery of 5-AVA and putrescine at the laboratory scale. While these results establish an improved and more reproducible framework for production, importantly, the host strain *C. glutamicum* and the separation methods used (ion-exchange and evaporation) are both industrially scalable, suggesting that the future adoption of lignocellulosic feedstocks could further enhance the economic and environmental sustainability of the process, aligning it with second generation biorefinery concepts.

4. Conclusion

This study presents a comprehensive and sustainable bioprocess for the microbial production and recovery of bio-based nylon monomers, marking a significant advance toward greener alternatives to petrochemical-derived polyamides. Through systematic optimization of medium composition and fermentation parameters, the production of 5-aminovaleric acid (5AVA) and putrescine was significantly improved. The application of response surface methodology *via* central composite design (CCD) led to a substantial enhancement in product titers, achieving 6.0 ± 0.28 g L^{-1} of 5AVA and 6.4 ± 0.33 g L^{-1} of putrescine. These results underscore the critical role of nutrient formulation particularly glucose, MOPS, and ammonium sulphate in maximizing microbial production efficiency in a defined minimal medium. Importantly, downstream recovery processes were developed with an emphasis on environmental compatibility and scalability. 5AVA was efficiently purified using ion exchange chromatography with Dowex 50W-X8 resin, achieving a high recovery yield of 84 ± 2% under mild, aqueous conditions. Putrescine was successfully concentrated to 14.32 ± 0.61 g L^{-1} through energy-efficient rotary evaporation. The integration of xylose and glucose co-utilization demonstrates the potential for leveraging lignocellulose-derived sugars, addressing one of the key challenges in second-generation biorefining. This work highlights a scalable microbial process for the recovery of high-value polymer precursors by valorising underutilized C5 sugars and minimizing the environmental footprint of production and purification. The process aligns with core green chemistry principles and contributes to the advancement of a circular, bio-based economy.

Conflicts of interest

The authors declare no conflicts of interest.

Data availability

The datasets supporting this study are available from the corresponding author upon reasonable request.

Supplementary information is available. Supplementary information: further discussion on the methodology and sample preparation for ICP-MS and additional details on the technoeconomic analysis. Tables included in the SI show the size range of olivine (Table S1), the composition of major cations in BPMED acid (Table S2), dissolution of olivine in mineral acid solutions of varying ionic strength (Table S3), solution volume lost to gel formation at different pH thresholds (Table S4), and cost estimates for major equipment needed for the proposed process (Table S5). Figures in the SI show EDS

analysis of olivine samples after 24 hours of dissolution (Fig. S1), photographs of the solution and solid residue from the bulk digestion experiment (Fig. S2), XRD of the solid residue after 2 weeks of digestion in BPMED acid (Fig. S3), photographs of the precipitates formed from pH adjustment (Fig. S4), the current profile of the electrodeposition (Fig. S5), XRD of the dried precipitates formed after pH adjustment (Fig. S6), photographs of the precipitate before and after heat treatment (Fig. S7), and XPS results from the electrodeposition experiment done before heat treatment (Fig. S8). See DOI: **https://doi.org/10.1039/d5su00799b**.

Acknowledgements

This work was supported by the grant from the Indo-German DBT BMBF project BIOCON. We would like to thank the DBT, New Delhi, and BMBF, Germany, for financial support. KS acknowledges the Council of Scientific and Industrial Research (CSIR) for providing a research fellowship.

References

1 S. Jae, E. Young, W. Noh, H. Min, Y. Hoon, S. Hwan, K. Song, J. Jegal and S. Yup, *Metab. Eng.*, 2013, **16**, 42–47.
2 P. Liu, H. Zhang, M. Lv, M. Hu, Z. Li, C. Gao and P. Xu, *Sci. Rep.*, 2014, 1–5.
3 J. S. Cho, K. J. Jeong, J. W. Choi, S. H. Park, J. C. Joo, S. J. Park, J. H. Shin, S. Y. Lee, J. Yu, M. H. Lee and Y. H. Oh, *Microb. Cell Fact.*, 2016, **15**, 1–13.
4 C. M. Rohles, G. Gießelmann, M. Kohlstedt, C. Wittmann and J. Becker, *Microb. Cell Fact.*, 2016, **15**, 1–13.
5 K. Sasikumar, S. Hannibal, V. F. Wendisch and K. M. Nampoothiri, *Front. Bioeng. Biotechnol.*, 2021, **9**, 1–9.
6 C. W. Tabor and H. Tabor, *Microbiol. Rev.*, 1985, **49**, 81–99.
7 M. Xuan, X. Gu, J. Li, D. Huang, C. Xue and Y. He, *Cell Commun. Signaling*, 2023, **21**, 1–24.
8 V. Pukin, C. G. Boeriu, E. L. Scott, J. P. M. Sanders and M. C. R. Franssen, *J. Mol. Catal. B:Enzym.*, 2010, **65**, 58–62.
9 J. Adkins, J. Jordan and D. R. Nielsen, *Biotechnol. Bioeng.*, 2013, **110**, 1726–1734.
10 L. Wang, G. Li and Y. Deng, *Appl. Environ. Microbiol.*, 2020, **86**, 1–15.
11 K. Thongbhubate, K. Irie, Y. Sakai, A. Itoh and H. Suzuki, *AMB Express*, 2023, **21**, 1–24.
12 J. Schneider and V. F. Wendisch, *Appl. Microbiol. Biotechnol.*, 2011, **91**, 17–30.
13 N. Mosier, C. Wyman, B. Dale, R. Elander, Y. Y. Lee, M. Holtzapple and M. Ladisch, *Bioresour. Technol.*, 2005, **96**, 673–686.
14 H. Kawaguchi, M. Sasaki, A. A. Vertès, M. Inui and H. Yukawa, *Appl. Microbiol. Biotechnol.*, 2006, **77**, 1053–1062.
15 Z. Zhao, M. Xian, M. Liu and G. Zhao, *Biotechnol. Biofuels*, 2020, **13**, 1–12.
16 V. Gopinath, T. M. Meiswinkel, V. F. Wendisch and K. M. Nampoothiri, *Appl. Microbiol. Biotechnol.*, 2011, **92**, 985–996.
17 Z. Zhong, Z. Ma, Y. Cao, H. Zhang, Y. Qi, L. Wei, J. Jiang, N. Xu and J. Liu, *ACS Sustain. Chem. Eng.*, 2025, **13**, 3441–3451.
18 H. T. Kim, K. A. Baritugo, S. M. Hyun, T. U. Khang, Y. J. Sohn, K. H. Kang, S. Y. Jo, B. K. Song, K. Park, I. K. Kim, Y. T. Hwang, S. Y. Lee, S. J. Park and J. C. Joo, *ACS Sustain. Chem. Eng.*, 2020, **8**, 129–138.
19 A. Burgardt, C. Prell and V. F. Wendisch, *Front. Bioeng. Biotechnol.*, 2021, **9**, 1–14.
20 J. M. P. Jorge, F. Pérez-garcía and V. F. Wendisch, *Bioresour. Technol.*, 2017, **245**, 1701–1709.
21 N. Hatambeygi, G. Abedi and M. Talebi, *J. Chromatogr. A*, 2011, **1218**, 5995–6003.
22 L. Switzar, M. Giera, H. Lingeman, H. Irth and W. M. A. Niessen, *J. Chromatogr. A*, 2011, **1218**, 1715–1723.
23 Q. D. Nguyen, J. Schneider, G. K. Reddy and V. F. Wendisch, *Metabolites*, 2015, **5**, 211–231.
24 K. Sasikumar, S. Hannibal, V. F. Wendisch and K. M. Nampoothiri, *Front. Bioeng. Biotechnol.*, 2021, **9**, 1–9.
25 M. Meeploy and R. Deewatthanawong, *J. Chromatogr. Sci.*, 2016, **54**, 445–452.
26 J. A. Lee, J. H. Ahn, I. Kim, S. Li and S. Y. Lee, *Chem. Eng. Sci.*, 2019, **196**, 324–332.
27 Y. Kabashima, J. I. Kishikawa, T. Kurokawa and J. Sakamoto, *J. Biochem.*, 2009, **146**, 845–855.
28 P. Yang, Y. Chen and A. dong Gong, *3 Biotech*, 2021, **11**, 1–10.
29 C. A. Lima, D. A. Viana Marques, B. B. Neto, J. L. Lima Filho, M. G. Carneiro-da-Cunha and A. L. F. Porto, *Biotechnol. Prog.*, 2011, **27**, 1470–1477.
30 S. Y. Lee and H. U. Kim, *Nat. Biotechnol.*, 2015, **33**, 1061–1072.
31 J. Chen, X. Lan, R. Jia, L. Hu and Y. Wang, *Microorganisms*, 2022, **10**, 1854–1871.
32 L. Chen, R. Li, X. Ren and T. Liu, *Bioresour. Technol.*, 2016, **214**, 138–143.
33 S. Puri, Q. K. Beg and R. Gupta, *Curr. Microbiol.*, 2002, **44**, 286–290.
34 J. Zhang and N. fa Gao, *J. Zhejiang Univ., Sci., B*, 2007, **8**, 98–104.
35 G. Gohari, S. Panahirad, M. Sadeghi, A. Akbari, E. Zareei, S. M. Zahedi, M. K. Bahrami and V. Fotopoulos, *BMC Plant Biol.*, 2021, **21**, 1–15.
36 S. Panahirad, M. Dadpour, G. Gohari, A. Akbari, G. Mahdavinia, H. Jafari, M. Kulak, R. Alcázar and V. Fotopoulos, *Plant Physiol. Biochem.*, 2023, **197**, 1–14.
37 V. F. Wendisch and J. Schneider, *Appl. Microbiol. Biotechnol.*, 2010, **88**, 859–868.
38 Z. G. Qian, X. X. Xia and S. Y. Lee, *Biotechnol. Bioeng.*, 2009, **104**, 651–662.
39 M. H. Cheng, H. Huang, B. S. Dien and V. Singh, *Biofuels, Bioprod. Biorefin.*, 2019, **13**, 723–739.